A Double-Transmitting Coil Wireless Power Transfer System Based on Parity Time Symmetry Principle

Hao Chen, Dongyuan Qiu, *Senior Member, IEEE*, Chao Rong, and Bo Zhang, *Senior Member, IEEE*

***Abstract*—The wireless power transfer (WPT) system based on parity-time (PT) symmetry has the advantages of robustness, stable, and efficient power transmission. However, the region of PT symmetry is limited, which cannot satisfy some practical requirements. Multiple transmitting coils have been shown to improve the misalignment tolerance of WPT systems. Towards this end, a parity-time-symmetric-based WPT (PT-based WPT) system with double-transmitting coil is presented in this article. First, an approximate equivalent circuit model of this PT-based WPT system was developed. Second, compared with the conventional single transmitting coil PT-based WPT system, the proposed system expands the PT symmetry region and provides higher output power and transmission efficiency. Furthermore, the mutual inductance between two transmitting coils can be designed to meet the requirements of different scenarios, which improves the freedom of system design. Finally, a 30 W prototype is designed to evaluate the proposed WPT system. Experimental results show that the critical coupling coefficient is reduced by about 12.5% at $k_{12} = 0.51$, which implies a longer transmission distance. Moreover, the maximum output voltage fluctuation in the strongly coupled region is only 3.5%, while the transfer efficiency is approximately constant, which implies stable and efficient power transfer.**

***Index Terms*—Mutual inductance, parity-time (PT) symmetry, transmitting coil, wireless power transfer (WPT).**

I. Introduction

WITH the advantages of electrical isolation, safety, and convenience, wireless power transfer technology has shown great potential for application in recent years in consumer electronics such as unmanned aerial vehicles [1], electric vehicles [2], [3], and implantable biomedical devices [4], [5].

In recent years, magnetic coupling resonance wireless power transfer (WPT) has stood out among many WPT technologies with its unique advantages, setting off a worldwide research upsurge [6]. The stable output of power is one of the application goals pursued by WPT technology. Unfortunately, magnetically coupled resonance WPT systems are not robust when mutual inductance varies, and thus fluctuations in transmission power and transmission efficiency occur. To obtain robust and efficient power transfer during mutual inductance varies, methods such as parameter estimation [7], [8], frequency tracking [9], [10], impedance matching [11], [12], and coupling coil optimization [13], [14], [15] can be used. However, most of these methods inevitably have the disadvantages of complex control and low transmission efficiency, and the system feedback control cannot be separated from the wireless communication between the transmitter and the receiver.

In 2017, the parity-time (PT) symmetric principle was introduced to WPT for the first time [16], providing an interdisciplinary solution to improve the robustness of WPT system. In the precise PT-symmetric region (also known as strong coupling region), the PT-based WPT can automatically select the operating frequency corresponding to the highest efficiency, thus ensuring robust power transfer over a wide range of coupling coefficients without any active tuning and feedback control. In PT-based WPT systems, the gain element used to provide power to the system is necessary. In [16], the nonlinear operational-amplifier was used as a gain element, however, this resulted in extremely low transmission efficiency as well as transmission power, which was not sufficient for practical applications. Subsequently, Strategies for the implementation of gain elements based on bridge inverters and class E inverters are presented in [17] and [18], [19], respectively, which greatly improve the transmission efficiency and transmission power of PT-based WPT systems [20], [21].

The robustness of the PT-based WPT system in the strongly coupled region is undeniably impressive, however, this is limited by the transmission distance. In [22], the transmission distance is enhanced by additional inductors on the receiver, which reduces the transmission efficiency and increases the size of the receiver. A high-order PT system using S/S/PS compensation is proposed in [23], which improves the transmission distance by reducing the equivalent load resistance of the receiver, however, this significantly reduces the transmission efficiency.

In addition, relay coils are commonly used to enhance the transmission distance of WPT systems [24]. In [25], [26], and [27], a PT system with relay coils is used to extend the transmission range. However, equal coupling coefficients between adjacent resonant cavities are necessary to be satisfied, which requires precise mechanical control and is difficult to achieve in practice. Multiple transmitting coils have been shown to improve the misalignment tolerance of WPT systems [28], [29], [30].

Manuscript received 27 March 2023; revised 22 June 2023; accepted 1 August 2023. Date of publication 9 August 2023; date of current version 22 September 2023. This work was supported by the Key Program of the National Natural Science Foundation of China under Grant 52130705. Recommended for publication by Associate Editor M. Liu. *(Corresponding author: Dongyuan Qiu.)*

The authors are with the School of Electric Power, South China University of Technology, Guangzhou 510640, China (e-mail: 202121016397@mail.scut.edu.cn; epdyqiu@scut.edu.cn; eprongchao@mail.scut.edu.cn; epbzhang@scut.edu.cn).

Color versions of one or more figures in this article are available at https://doi.org/10.1109/TPEL.2023.3303613.

Digital Object Identifier 10.1109/TPEL.2023.3303613

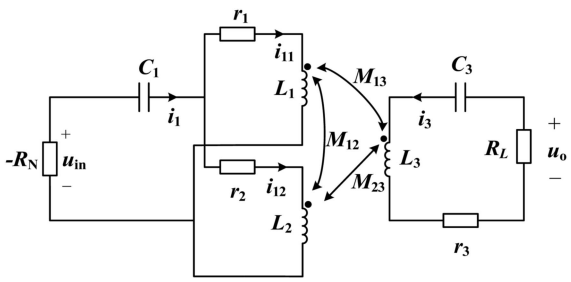

Fig. 1. Equivalent circuit of PT-based WPT system with double transmitting coils.

In [29], a WPT system with triple decoupled transmit coil is proposed to improve the coupling stability by controlling the phase of the primary current. The flux distribution of different pads was compared in [30], and the results showed that the multicoil pad can enhance the misalignment tolerance of the system in different orientations. On this basis, a three-mode pseudo-Hermitian dual-transmitter-single-receiver system is proposed in [31], which can achieve frequency-stable high-efficiency power transfer in the strong coupling region, yet the transmission power fluctuates considerably with coupling coefficient.

To address the abovementioned issues, this article proposes a WPT system with double transmitting coils based on the PT symmetry principle. The main works and contributions are summarized as follows.

1) A PT-based WPT system with double transmitting coils is proposed by introducing the PT-symmetry principle into the multitransmission coil system. This PT-based WPT system can effectively reduce the critical coupling coefficient and improve the transmission efficiency as well as the transmission power.
2) An approximate simplified model of the proposed PT-based WPT system is developed, and the approximate system operating conditions and transmission characteristics are obtained by this model. Moreover, the feasibility of the approximation condition is demonstrated.
3) The coupling between two transmitting coils can be adjusted to meet the requirements of different practical application scenarios.

The rest of this article is organized as follows. In Section II, the circuit model of the proposed system is established, then the feasibility of approximation treatment is analyzed. In Section III, the proposed system is compared with the single transmitting coil PT-based WPT system. In Section IV, the control strategy and hardware scheme are introduced, and a 30 W prototype is built. Finally, Section V concludes this article.

II. Theoretical Analysis and Modeling

A. System Modeling and Analysis

Different from the conventional PT-based WPT system with a single transmitter coil, this proposed system is equipped with double transmitting coils. Fig. 1 shows the equivalent circuit of the PT-based WPT system with double transmitting coils, where negative resistance -$R_{\rm N}$ is used to provide input power to the system, and the corresponding input voltage is $u_{\rm in}$. L_1 and L_2 represent the self-inductances of the double transmitting coils, respectively. r_1, r_2 represents their internal resistance, respectively. L_3 and r_3 represent the self-inductance and internal resistance of the receiver coil. In this article, two transmitting coils are assumed to be completely symmetrical, i.e., $L_1 = L_2$, $r_1 = r_2$. M_{12} is the mutual inductance between the two transmitting coils, M_{13} and M_{23} are the mutual inductance between the two transmitting coils and the receiving coils, respectively. k_{ij} represents the coupling coefficient corresponding to M_{ij}, and $k_{ij} = \frac{M_{ij}}{\sqrt{L_i L_j}}$ $(i, j = 1, 2, 3, i \neq j)$. C_1, C_3 are the compensating capacitors for the transmitter and the receiver, respectively. R_L is the equivalent load resistance, and u_o is the output voltage.

Based on the circuit theory, suppose $X_1 = \omega L_1 - \frac{1}{\omega C_1}$, $X_3 = \omega L_3 - \frac{1}{\omega C_3}$, the circuit model of PT-based WPT system proposed in this article can be expressed as

$$\begin{bmatrix} r_1 - R_N + jX_1 & -R_N + \frac{1}{j\omega C_1} + j\omega M_{12} & j\omega M_{13} \\ -R_N + \frac{1}{j\omega C_1} + j\omega M_{12} & r_2 - R_N + \frac{1}{j\omega C_1} + j\omega L_2 & j\omega M_{23} \\ j\omega M_{13} & j\omega M_{23} & r_3 + R_L + jX_3 \end{bmatrix} \times \begin{bmatrix} \dot{I}_{11} \\ \dot{I}_{12} \\ \dot{I}_3 \end{bmatrix} = 0. \tag{1}$$

Then, the operating frequency ω can be determined by the following characteristic equation:

$$\begin{vmatrix} r_1 - R_N + X_1 & -R_N + \frac{1}{j\omega C_1} + j\omega M_{12} & j\omega M_{13} \\ -R_N + \frac{1}{j\omega C_1} + j\omega M_{12} & r_2 - R_N + \frac{1}{j\omega C_1} + j\omega L_2 & j\omega M_{23} \\ j\omega M_{13} & j\omega M_{23} & r_3 + R_L + X_3 \end{vmatrix} = 0. \tag{2}$$

The compensation capacitors C_1, C_3 are determined by (3), where ω_0 is the resonance frequency of the system. Since the position of the transmitter is fixed and no longer move, the values of the compensation capacitance C_1 and C_3 can be considered fixed

$$C_1 = \frac{2}{\omega_0^2 L_1 (1 + k_{12})}, C_3 = \frac{1}{\omega_0^2 L_3} \tag{3}$$

Based on (3), (2) can be reduced to (4) shown at the bottom of the next page, where $a = 2 - \frac{1}{\varepsilon}$, $\varepsilon = \frac{1 - k_{12}}{(k_{13} - k_{23})^2}$. When k_{13} and k_{23} are close, a can be approximated by

$$a = 2 - \frac{1}{\varepsilon} \approx 2. \tag{5}$$

Based on (5), (4) can be simplified as

$$(\omega^2 - \omega_0^2)\left(\left(1 - \frac{2k^2}{k_{12} + 1}\right)\frac{\omega^4}{\omega_0^4} + \frac{\omega^2}{\omega_0^2}\left(\frac{(R_L + r_3)^2}{\omega_0^2 L_3^2} - 2\right) + 1\right) = 0 \tag{6}$$

where $k = \sqrt{k_{13} k_{23}}$ is defined as the equivalent coupling coefficient.

The steady-state solution of ω is

$$\omega = \begin{cases} \omega_0, k < k_c \\ \omega_{1,2} = \omega_0 \sqrt{\frac{\gamma \pm \sqrt{\gamma^2 - 4b}}{2b}}, k \geq k_c \end{cases} \tag{7}$$

where $k_c = \beta\sqrt{1 - \frac{\gamma^2}{4}}$ is the critical coupling coefficient of the system and $\beta = \sqrt{\frac{1+k_{12}}{2}}$, $\gamma = 2 - (\frac{r_3 + R_L}{\omega_0 L_3})^2$, $b = 1 - \frac{2k^2}{1+k_{12}}$.

From (7), the system stable operation region is divided into the strong coupling region (i.e., $k \geq k_c$) and the weak coupling region (i.e., $k < k_c$). In the strong coupling region, the system automatically oscillates at $\omega_{1,2}$, while in the weak coupling region there is only one real number solution, ω_0 [17]. Furthermore, it can be seen from (7) that the value of k_{12} can be adjusted to obtain different k_c, thus adapting to different application scenarios.

B. Transmission Characteristics Analysis

When the system is in the strongly coupled region, the negative resistance R_N and current gain I_3/I_1 are obtained by substituting (5) and (7) into (2) and (1), respectively, as follows:

$$R_N = \frac{L_1 (r_3 + R_L) \beta^2}{L_3} + \frac{1}{2} r_1 \tag{8}$$

$$\frac{I_3}{I_1} = \beta \sqrt{\frac{L_1}{L_3}}. \tag{9}$$

In the strongly coupled region, load estimation can be performed on the primary side according to (8) without any wireless communication as well as feedback control, which is advantageous for applications requiring constant voltage and constant current charging.

In addition, it can be seen from (9) that the current gain I_3/I_1 is independent of k_{13} and k_{23} in the strong coupling region. The voltage gain U_o/U_{in} can be obtained by

$$\frac{U_o}{U_{in}} = \frac{I_3 R_L}{I_1 R_N} = \frac{R_L}{(r_3 + R_L)\beta \sqrt{\frac{L_1}{L_3}} + \frac{r_1}{2\beta}\sqrt{\frac{L_3}{L_1}}}. \tag{10}$$

According to (9) and (10), the output power P_o and transmission efficiency η are determined by

$$\eta = \frac{I_3^2 R_L}{I_1^2 R_N} = \frac{R_L}{\frac{L_3}{2\beta^2 L_1} r_1 + r_3 + R_L} \tag{11}$$

$$P_o = \frac{U_o^2}{R_L} = \frac{R_L U_{in}^2}{\frac{\beta^2 L_1}{L_3}(r_3 + R_L)^2 + \frac{L_3 r_1^2}{4\beta^2 L_1} + (r_3 + R_L) r_1}. \tag{12}$$

From (10) to (12), it can be seen that the output voltage, transmission efficiency, and transmission power of the proposed system are independent of the coupling coefficient in the strong coupling region.

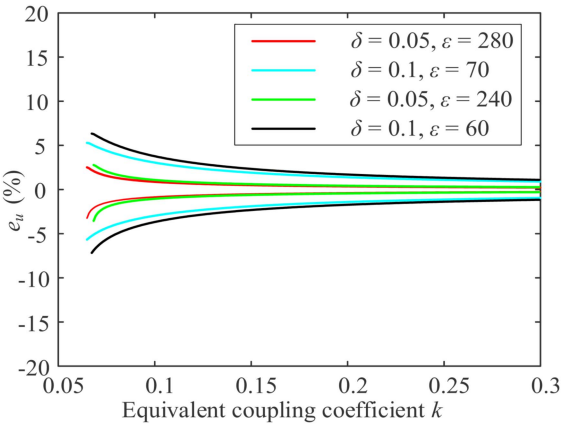

Fig. 2. Approximate deviations of output voltage when $k_{13} \neq k_{23}$.

C. Feasibility Analysis When $k_{13} \neq k_{23}$

In practical, the different positions of coupling coils will result in (5) not being satisfied, which will introduce errors into the theoretical analysis. Let $\delta = k_{13} - k_{23}$ when assuming $k_{13} \geq k_{23}$. In order to verify the impact of δ on the theoretical analysis of the system, the deviations of the output voltage under different values of δ and ε are given in Fig. 2, where the normalized output voltage error e_u is defined by $e_u = \frac{(U_o)_{\delta \neq 0} - (U_o)_{\delta = 0}}{(U_o)_{\delta = 0}}$. The other parameters used in the Fig. 2 are $L_1 = L_2 = L_3 = 272\ \mu$H, $r_1 = r_2 = r_3 = 0.65\ \Omega$, $R_o = 20\ \Omega$, $f_0 = 150$ kHz, $k_{23} = \frac{-\delta + \sqrt{\delta^2 + 4k^2}}{2}$, and $k_{13} = k_{23} + \delta$.

As can be seen from Fig. 2, first of all, the theoretical error increases with decreasing ε, but it is mainly concentrated near the critical coupling coefficient, which is mainly due to the slight shift of the actual critical coupling coefficient. Second, when $\delta = 0.1$, $\varepsilon = 60$, corresponding to $k_{13} = 0.134$, $k_{23} = 0.034$, e_u reaches a maximum of 7.17% at this point, which means that the system is still robust in $k_{13} \neq k_{23}$. Finally, e_u can be reduced by increasing ε, which can be achieved by coupling mechanism optimization.

III. Analysis and Comparison of Transmission Characteristics

To further illustrate the advantages of the proposed structure, Table I gives a comparison of the transmission characteristics of the PT-based WPT systems with single and double transmitting

$$\omega^2 \left\{ \left(1 + \frac{a-2}{k_{12}+1} - \frac{2k_{13}k_{23}}{k_{12}+1}\right) \frac{\omega^4}{\omega_0^4}(a\omega^2 - 2\omega_0^2) + \frac{\omega^2}{\omega_0^2} \left(\frac{2(R_L + r_3)^2(\omega^2 - \omega_0^2)}{\omega_0^2 L_3^2} - (a+2)\left(\frac{a}{2}\omega^2 - \omega_0^2\right) \right) + (a\omega^2 - 2\omega_0^2) \right\}$$
$$+ \frac{r_1^2}{L_1^2} \frac{(\omega^2 - \omega_0^2)}{(k_{12}-1)^2} \left(\left(2 - \frac{(a-2)(k_{12}-1) + 4k_{13}k_{23}}{1+k_{12}}\right) \frac{\omega^4}{\omega_0^4} + 2\frac{R_L^2}{\omega_0^2 L_3^2}\frac{\omega^2}{\omega_0^2} - 4\frac{\omega^2}{\omega_0^2} + 2 \right) + \frac{2r_1 R_L}{L_1 L_3}\frac{\omega^4}{\omega_0^4}\frac{(a-2)(\omega^2 - \omega_0^2)}{k_{12}+1} = 0. \tag{4}$$

TABLE I
PERFORMANCE COMPARISON BETWEEN THE PROPOSED SYSTEM WITH DOUBLE TRANSMITTING COIL AND THE CONVENTIONAL SYSTEM WITH SINGLE TRANSMITTING COIL

Quantity of transmitting coil	Equivalent circuit	Critical coupling coefficient k_c	Output power P_o	Transfer efficiency η
Single	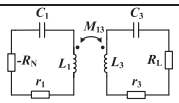	$\sqrt{1-\frac{1}{4}\gamma^2}$	$\frac{R_L U_{in}^2}{\frac{L_1}{L_3}(r_3+R_L)^2+\frac{L_3}{L_1}r_1^2+2r_1(r_3+R_L)}$	$\frac{R_L}{\frac{L_3}{L_1}r_1+r_3+R_L}$
Double	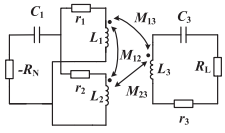	$\beta\sqrt{1-\frac{1}{4}\gamma^2}$	$\frac{R_L U_{in}^2}{\frac{\beta^2 L_1}{L_3}(r_3+R_L)^2+\frac{L_3}{4\beta^2 L_1}r_1^2+r_1(r_3+R_L)}$	$\frac{R_L}{\frac{L_3}{2\beta^2 L_1}r_1+r_3+R_L}$

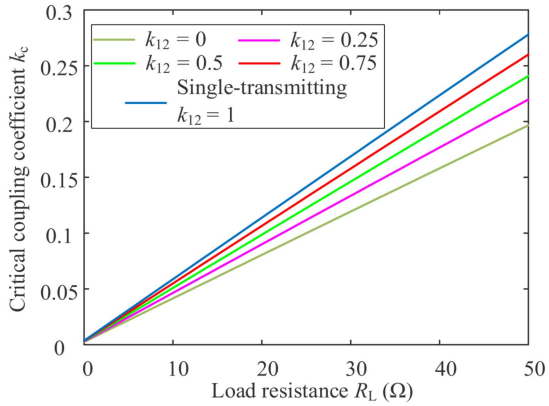

Fig. 3. Critical coupling coefficient versus load.

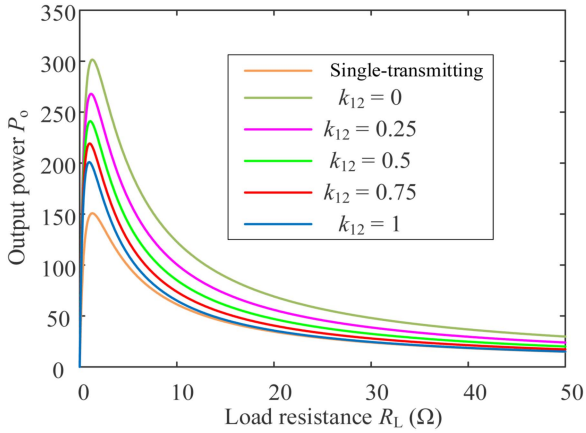

Fig. 4. Output power versus load.

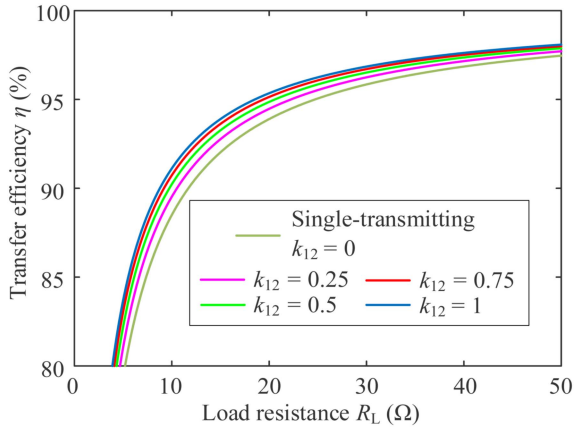

Fig. 5. Transfer efficiency versus load.

coils, respectively. It can be seen that the critical coupling coefficient of the double transmitting coils system is reduced by a factor of β compared to the single transmitting coil system, which implies a longer transmission distance. In addition, for the same parameters, higher efficiency and transmission power can be obtained with the proposed structure without sacrificing the size of the receiver.

Then, to make the comparison more intuitive, the corresponding transmission characteristic can be obtained by means of the expressions in Table I. From Figs. 3, 4, and 5, it can be seen that the transmission efficiency of the proposed system was the same as the single transmitting PT-WPT system at $k_{12}=0$, while the critical coupling coefficients of both are the same at $k_{12}=1$. Furthermore, the critical coupling coefficient decreases and the output power increases as k_{12} decreases, while the transmission efficiency decreases slightly. Therefore, k_{12} can be reasonably selected to meet the requirements of different application scenario.

IV. EXPERIMENTAL VERIFICATION

A. Implementation of Negative Resistance

The realization of negative resistance is crucial to the operation of the system. In the previous work, several methods have been proposed to realize the negative resistance, including nonlinear operational amplifier [16], self-excited oscillation control bridge inverter [17], and Class E inverter [18], [19]. The self-excited oscillation control strategy has the advantages of simple control and high efficiency. Therefore, the self-excited oscillation method is used in this work to control the full-bridge inverter and realize the negative resistance. Its control strategy and detailed hardware implementation scheme are shown in Fig. 6(a) and (b), respectively. First, the output current of the full-bridge inverter is sampled by the current transformer

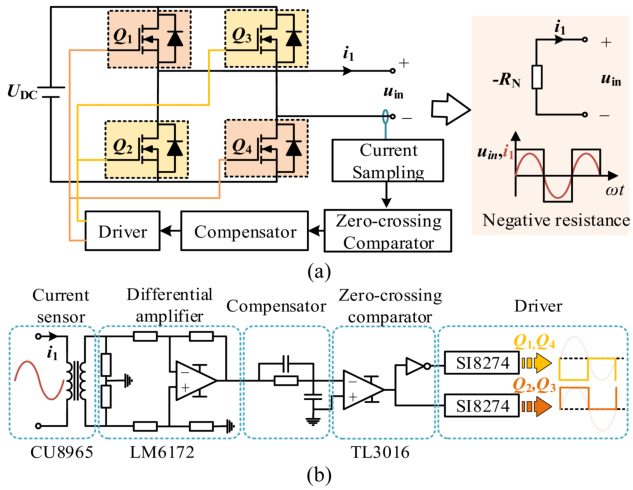

Fig. 6. Self-excited oscillation control strategy for negative resistance. (a) Equivalent circuit. (b) Controller implementation.

TABLE II
PARAMETERS OF THE PROTOTYPE

Symbol	Values
L_1	274 μH
L_2	274 μH
L_3	272 μH
C_1	5.371 nF
C_3	4.139 nF
r_1	0.69 Ω
r_2	0.7 Ω
r_3	0.65 Ω
R_o	30 Ω
f_0	150 kHz
U_{DC}	28 V

CU9865, then it passes through the zero-crossing comparator TL3016 to generate the rectangular control signal, and eventually the drivers SI8274 is used to control Q_1–Q_4. Moreover, the fundamental component of the output voltage can be deduced as

$$U_{in} = \frac{2\sqrt{2}U_{DC}}{\pi}. \tag{13}$$

B. Experimental Setup

A 30 W experimental prototype with parameters listed in Table II is constructed, and its circuit equivalent is shown in Fig. 7(a), where the rectifier is composed by D_1–D_4, C_f is the filter capacitor of the rectifier, R_o is the load resistance of the rectifier, and $R_L = 8R_o/\pi^2$. The experimental prototype is shown in Fig. 7(b), where both the transmitter and receiver adopt the same size planar coiled coil structure and are tightly coiled by the Litz wire (0.05 mm diameter, 800 strands). The outer and inner diameters of the coil are 350 mm and 243 mm, respectively. Receiving coil is placed individually, and the two transmitting coils were placed in stack to obtain proper mutual inductance,

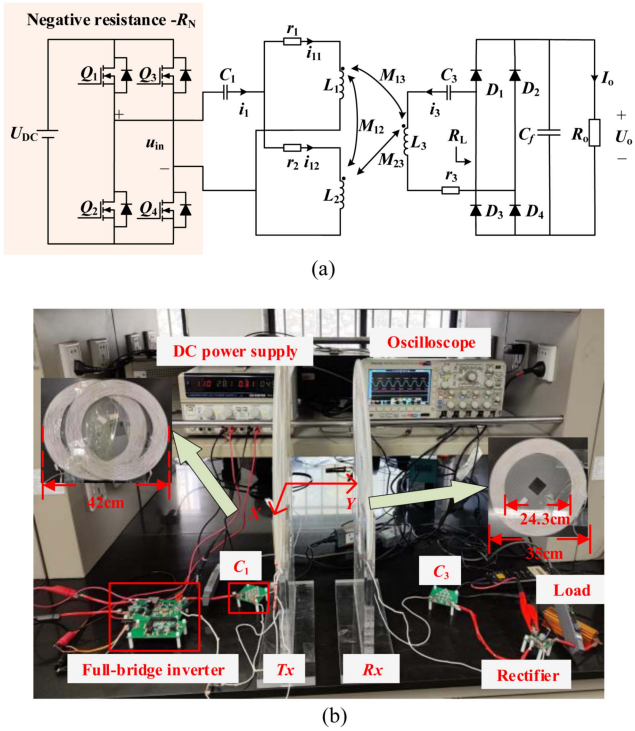

Fig. 7. PT-based WPT with double transmitting coils. (a) Overall equivalent circuit. (b) Experimental prototype.

the coupling coefficient k_{12} is 0.53, which was measured by a precision impedance analyzer (Wayne Kerr 6500B). Fig. 8 shows the variation of the coupling coefficients k_{13}, k_{23}, and k when the coils are misaligned in the X- and Y-directions, respectively. It can be seen that k decreases more slowly when misaligned in the X-direction compared to misalignment in the Y-direction. Moreover, the variations of the coupling coefficients almost overlap when misaligned in the Y-direction due to the symmetry of the double transmitting coils.

C. Experimental Results

Fig. 9 shows the variation of the operating frequency of the prototype when the position of the receiver coil changes. Based on Table I, it can be obtained that $k_c = 0.0851$ when $R_o = 30\ \Omega$, which is 12.5% lower compared to 0.0973 for the single transmitter coil PT-based WPT system, effectively improving the transmission distance. Besides, when $k < k_c$, the operating frequency fluctuates around the resonant frequency, while when $k \geq k_c$, the experimental frequency varies mainly around the high frequency branch, which is consistent with the theoretical analysis.

Fig. 10 shows the experimental waveforms when X-direction misalignment occurs. The experimental results show that the input voltage source can always be approximately equivalent to a negative resistance, which verify the effectiveness of the self-oscillation strategy in Section IV. Fig. 11 shows the output voltage gain as well as transmission efficiency at X-direction coil offset, and it can be seen that the transfer efficiency as well as voltage gain appears to inflection at approximately $\Delta X =$

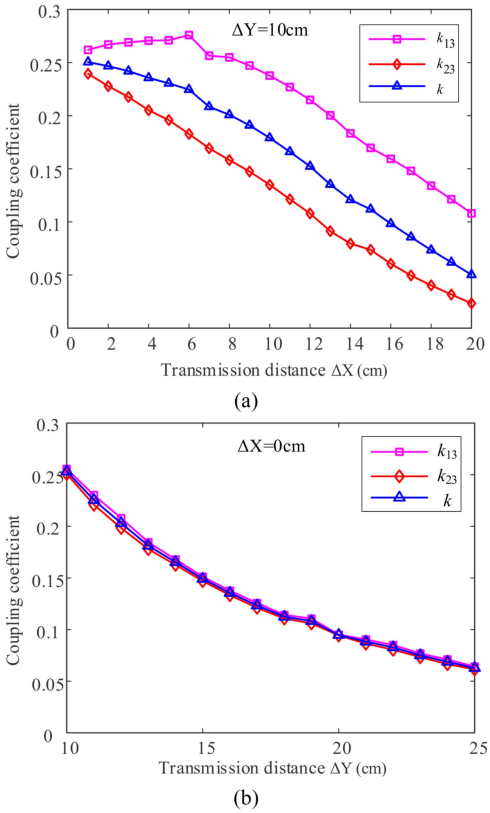

Fig. 8. Coupling coefficient versus transmission distance. (a) Coil misalignment in *X*-direction. (b) Coil misalignment in *Y*-direction.

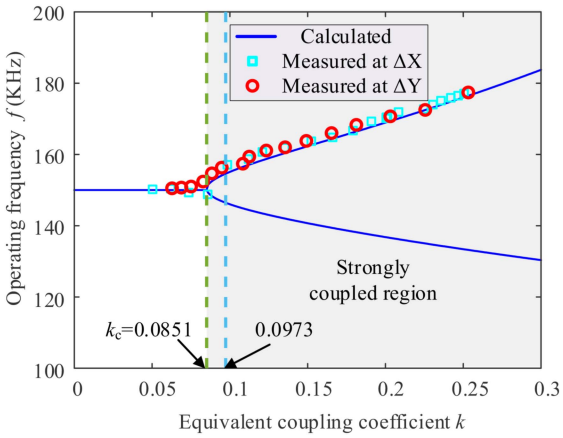

Fig. 9. Experimental operating frequency.

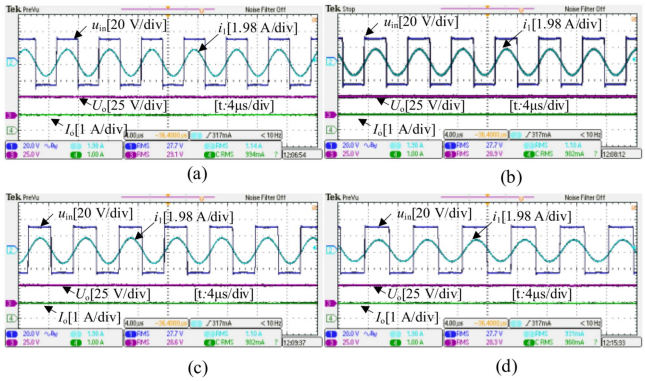

Fig. 10. Experimental waveforms of coil *X*-direction misalignment. (a) ΔX = 4 cm. (b) ΔX = 8 cm. (c) ΔX = 12 cm. (d) ΔX = 16 cm.

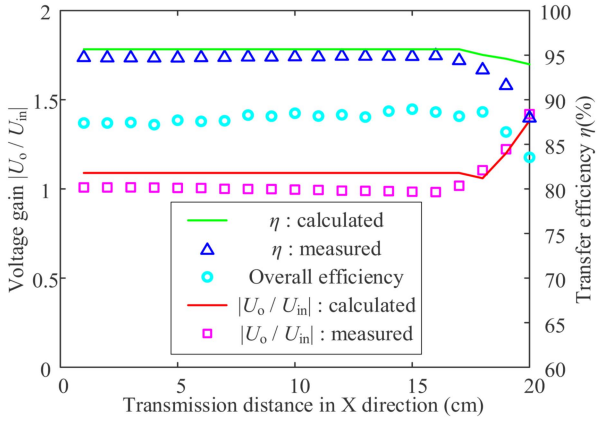

Fig. 11. Voltage gain and transfer efficiency in *X*-direction misalignment.

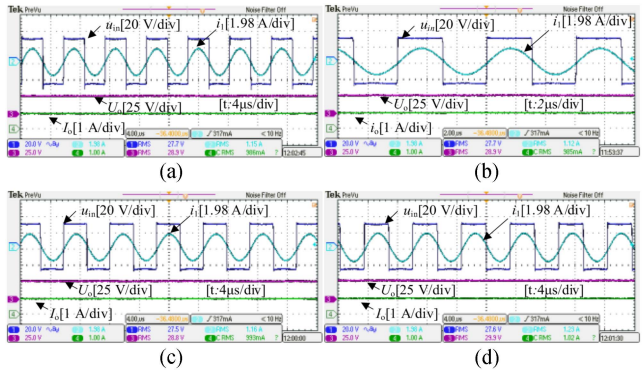

Fig. 12. Experimental waveforms of coil *Y*-direction misalignment. (a) ΔY = 10 cm. (b) ΔY = 14 cm. (c) ΔY = 18 cm. (d) ΔY = 22 cm.

17 cm, at which point the corresponding equivalent coupling coefficient k is actually 0.0858, the theoretical value is 0.0851, and the theoretical value is close to the actual value. Also, it can be seen from Figs. 8 and 11 that there is $k_{13} \neq k_{23}$ when the coils are misaligned in the *X*-direction, while the maximum fluctuation of output voltage and transfer efficiency within $k \geq k_c$ is only 3.5% and 0.55%, respectively, while the overall efficiency varies between 87.2% and 88.9%.

To further verify the correctness of the theoretical analysis, Figs. 12 and 13 show the experimental waveforms, output voltage gain and transmission efficiency of the prototype when the *Y*-direction misalignment occurs. It can be seen that the input voltage and input current can remain in phase when the coil is misaligned. Additional, when ΔY ≥ 22 cm, the system enters the weak coupling region, where the corresponding equivalent coupling coefficient k is 0.0828, the theoretical value is 0.0851,

TABLE III
COMPARISON OF EXISTING WPT SYSTEMS

Method	Reference	Coil number/ Compensation Topology	Transfer distance(cm)	Output power(W)	Transfer efficiency	Increased receiver volume
Class E power amplifier and rectifier	[18]	2/SP	65	9	92%	No
	[19]	2/SS	12	165	92.6%	Yes
High-order compensation	[22]	2/C-LLC	26.6	156.7	87.4%	Yes
	[23]	3/S-S-PS	30	38	85%	Yes
Relay Coil	[25]	3/S-S-S	42	15	91%	Yes
		4/S-S-S-S	50		89%	Yes
	[26]	3/S-S-S	20-60	N/A	40%–80%	Yes
	[31]	3/P-P-P	3.8	N/A	82%–89%	No
Multi-transmission coil	This paper	3/SS	x=0, y=0–22 x=0–17, y=10	28	94.2%–94.9%	No

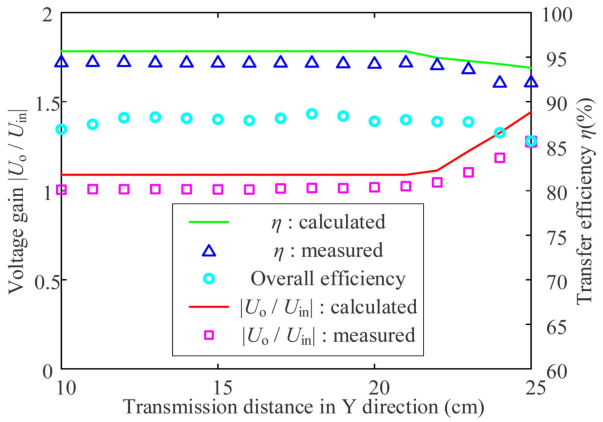

Fig. 13. Voltage gain and transfer efficiency in *Y*-direction misalignment.

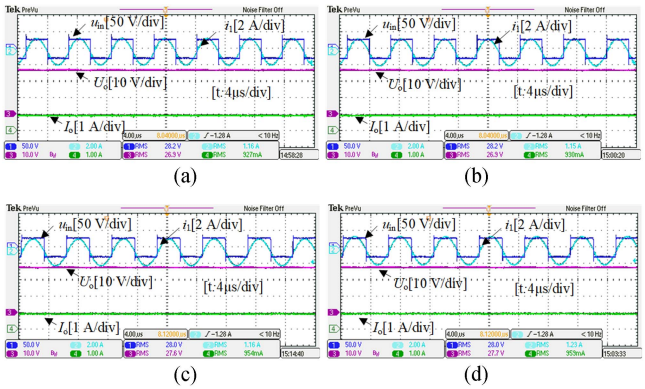

Fig. 14. Experimental waveforms when $k_{12} = 0.84$. (a) $\Delta X = 0$ cm, $\Delta Y = 10$ cm. (b) $\Delta X = 5$ cm, $\Delta Y = 10$ cm. (c) $\Delta X = 0$ cm, $\Delta Y = 15$ cm. (d) $\Delta X = 5$ cm, $\Delta Y = 15$ cm.

and the theoretical value is close to the actual value. When $\Delta Y < 22$ cm, the maximum fluctuation of output voltage gain is 2%, which is smaller than the misalignment fluctuation in *X*-direction, mainly due to the smaller δ in *Y*-direction misalignment. Finally, the transmission efficiency of the system is always higher than 94% in the strongly coupled region, and the overall efficiency is around 88%, which achieves robust and efficient power transmission. The experimental results are in accordance with the theoretical analysis.

Fig. 14 shows the experimental waveforms of coil misalignment in different directions when $k_{12} = 0.84$. It can be seen that an increase in k_{12} brings about a decrease in transfer power compared to $k_{12} = 0.53$ in Figs. 10 to 13. However, as can be seen in Fig. 5, a larger k_{12} implies a higher transmission efficiency. Furthermore, the variation of the system output voltage is within 3% for various coil misalignments, which verifies the correctness of the theoretical analysis.

Table III compares the transmission characteristics of several WPT systems issued in recent years. It can be seen that the PT-WPT system with double-transmitting coil proposed in this article has competitive advantages in terms of transfer distance, transfer efficiency, and transfer power and without increasing the volume of the receiver.

V. CONCLUSION

In order to improve the antimisalignment capability of WPT system, a PT-based WPT system with double transmitting coils is presented. Although the double transmitting coil structure increases the complexity of the system model, a simplified system model is proposed by approximate equivalent method, and on this basis, the frequency, transmission efficiency, transmission power, and other analytical equations are obtained. Compared with the single transmitting coil PT-based WPT system, the proposed system improves the transmission distance, increases the transmission power and transmission efficiency, and ensures the compactness and light weight of the receiver. The feasibility of the approximate equivalent method proposed in this article was verified by coil misalignment experiments, which showed that the maximum fluctuation of output voltage gain within the strongly coupled region was only about 3.5%, and the transmission efficiency was always stable above 94%. Finally, the transmitter can be designed to obtain different coupling coefficients k_{12}, which can meet the requirements of transmission power and transmission efficiency in different application scenarios. With a coupling coefficient of $k_{12} = 0.53$, the strongly coupled region of the double transmitter system is extended by about 12.5% compared to the conventional single transmitter PT-based WPT system.

REFERENCES

[1] Z. Li, H. Liu, Y. Tian, and Y. Liu, "Constant current/voltage charging for primary-side controlled wireless charging system without using dual-side communication," *IEEE Trans. Power Electron.*, vol. 36, no. 12, pp. 13562–13577, Dec. 2021.

[2] S. Y. Chu, X. Cui, X. Zan, and A.-T. Avestruz, "Transfer-power measurement using a non-contact method for fair and accurate metering of wireless power transfer in electric vehicles," *IEEE Trans. Power Electron.*, vol. 37, no. 2, pp. 1244–1271, Feb. 2022.

[3] Y. Zhang, Z. Shen, W. Pan, H. Wang, Y. Wu, and X. Mao, "Constant current and constant voltage charging of wireless power transfer system based on three-coil structure," *IEEE Trans. Ind. Electron.*, vol. 70, no. 1, pp. 1066–1070, Jan. 2023.

[4] T. Campi, S. Cruciani, F. Maradei, A. Montalto, F. Musumeci, and M. Feliziani, "Centralized high power supply system for implanted medical devices using wireless power transfer technology," *IEEE Trans. Med. Robot. Bionics*, vol. 3, no. 4, pp. 992–1001, Nov. 2021.

[5] G. L. Barbruni, P. M. Ros, D. Demarchi, S. Carrara, and D. Ghezzi, "Miniaturised wireless power transfer systems for neurostimulation: A review," *IEEE Trans. Biomed. Circuits Syst.*, vol. 14, no. 6, pp. 1160–1178, Dec. 2020.

[6] A. Kurs, A. Karalis, R. Moffatt, J. D. Joannopoulos, and M. Soljacic, "Wireless power transfer via strongly coupled magnetic resonances," *Science*, vol. 317, no. 5834, pp. 83–86, 2007.

[7] Y.-G. Su, L. Chen, X.-Y. Wu, A. P. Hu, C.-S. Tang, and X. Dai, "Load and mutual inductance identification from the primary side of inductive power transfer system with parallel-tuned secondary power pickup," *IEEE Trans. Power Electron.*, vol. 33, no. 11, pp. 9952–9962, Nov. 2018.

[8] J. Liu, G. Wang, G. Xu, J. Peng, and H. Jiang, "A parameter identification approach with primary-side measurement for DC–DC wireless-power-transfer converters with different resonant tank topologies," *IEEE Trans. Transp. Electrific.*, vol. 7, no. 3, pp. 1219–1235, Sep. 2021.

[9] J. P.-W. Chow, H. S.-H. Chung, and C.-S. Cheng, "Use of transmitter-side electrical information to estimate mutual inductance and regulate receiver-side power in wireless inductive link," *IEEE Trans. Power Electron.*, vol. 31, no. 9, pp. 6079–6091, Sep. 2016.

[10] D.-W. Seo and J.-H. Lee, "Frequency-tuning method using the reflection coefficient in a wireless power transfer system," *IEEE Microw. Wireless Compon. Lett.*, vol. 27, no. 11, pp. 959–961, Nov. 2017.

[11] H. Shui, D. Yu, S. Yu, H. H. C. Iu, T. Fernando, and H. Cheng, "An autonomous impedance adaptation strategy for wireless power transfer system using phase-controlled switched capacitors," *IEEE J. Emerg. Sel. Topics Power Electron.*, vol. 9, no. 2, pp. 2303–2316, Apr. 2021.

[12] Y. Shao, H. Zhang, M. Liu, and C. Ma, "Explicit design of impedance matching networks for robust MHz WPT systems with different features," *IEEE Trans. Power Electron.*, vol. 37, no. 9, pp. 11382–11393, Sep. 2022.

[13] F. Wen, X. Cheng, Q. Li, W. Zhao, X. Zhu, and Y. Wu, "A strong misalignment tolerance dual-channel coupler for wireless power transfer system," *IEEE Trans. Appl. Supercond.*, vol. 31, no. 8, Nov. 2021, Art. no. 0601005.

[14] Y. Zhuang, A. Chen, C. Xu, Y. Huang, H. Zhao, and J. Zhou, "Range-adaptive wireless power transfer based on differential coupling using multiple bidirectional coils," *IEEE Trans. Ind. Electron.*, vol. 67, no. 9, pp. 7519–7528, Sep. 2020.

[15] Y. Wang, P. Gu, Y. Yao, and D. Xu, "Analysis and design of cubic magnetic coupler for high distance-to-diameter ratio IPT systems," *IEEE Trans. Ind. Electron.*, vol. 69, no. 1, pp. 409–419, Jan. 2022.

[16] S. Assawaworrarit, X. Yu, and S. Fan, "Robust wireless power transfer using a nonlinear parity–Time-symmetric circuit," *Nature*, vol. 546, no. 7658, pp. 387–390, Jun. 2017.

[17] J. Zhou, B. Zhang, W. Xiao, D. Qiu, and Y. Chen, "Nonlinear parity-time-symmetric model for constant efficiency wireless power transfer: Application to a drone-in-flight wireless charging platform," *IEEE Trans. Ind. Electron.*, vol. 66, no. 5, pp. 4097–4107, May 2019.

[18] S. Assawaworrarit and S. Fan, "Robust and efficient wireless power transfer using a switch-mode implementation of a nonlinear parity–Time symmetric circuit," *Nature Electron.*, vol. 3, no. 5, pp. 273–279, May 2020.

[19] L. He, X. Huang, and B. Cheng, "Robust class E^2 wireless power transfer system based on parity–Time symmetry," *IEEE Trans. Power Electron.*, vol. 38, no. 4, pp. 4279–4288, Apr. 2023.

[20] L. Wu, B. Zhang, and Y. Jiang, "Position-independent constant current or constant voltage wireless electric vehicles charging system without dual-side communication and DC–DC converter," *IEEE Trans. Ind. Electron.*, vol. 69, no. 8, pp. 7930–7939, Aug. 2022.

[21] L. Wu, B. Zhang, Y. Jiang, and J. Zhou, "A robust parity-time-symmetric WPT system with extended constant-power range for cordless kitchen appliances," *IEEE Trans. Ind. Appl.*, vol. 58, no. 1, pp. 1179–1189, Jan./Feb. 2022.

[22] Z. Wei and B. Zhang, "Transmission range extension of PT-symmetry-based wireless power transfer system," *IEEE Trans. Power Electron.*, vol. 36, no. 10, pp. 11135–11147, Oct. 2021.

[23] Y. Qu, B. Zhang, W. Gu, and X. Shu, "Wireless power transfer system with high-order compensation network based on parity-time-symmetric principle and relay coil," *IEEE Trans. Power Electron.*, vol. 38, no. 1, pp. 1314–1323, Jan. 2023.

[24] D.-W. Seo, "Comparative analysis of two-and three-coil WPT systems based on transmission efficiency," *IEEE Access*, vol. 7, pp. 151962–151970, 2019.

[25] X. Shu, B. Zhang, Z. Wei, C. Rong, and S. Sun, "Extended-distance wireless power transfer system with constant output power and transfer efficiency based on parity-time-symmetric principle," *IEEE Trans. Power Electron.*, vol. 36, no. 8, pp. 8861–8871, Aug. 2021.

[26] C. Zeng et al., "High-order parity-time symmetric model for stable three-coil wireless power transfer," *Phys. Rev. Lett.*, vol. 13, no. 3, Mar. 2020, Art. no. 034054.

[27] M. Sakhdari, M. Hajizadegan, and P.-Y. Chen, "Robust extended-range wireless power transfer using a higher-order PT-symmetric platform," *Phys. Rev. Res.*, vol. 2, no. 1, Feb. 2020, Art. no. 013152.

[28] Y. Zhang et al., "Misalignment-tolerant dual-transmitter electric vehicle wireless charging system with reconfigurable topologies," *IEEE Trans. Power Electron.*, vol. 37, no. 8, pp. 8816–8819, Aug. 2022.

[29] S. Kim, G. A. Covic, and J. T. Boys, "Tripolar pad for inductive power transfer systems for EV charging," *IEEE Trans. Power Electron.*, vol. 32, no. 7, pp. 5045–5057, Jul. 2017.

[30] A. Zaheer, H. Hao, G. A. Covic, and D. Kacprzak, "Investigation of multiple decoupled coil primary pad topologies in lumped IPT systems for interoperable electric vehicle charging," *IEEE Trans. Power Electron.*, vol. 30, no. 4, pp. 1937–1955, Apr. 2015.

[31] X. Hao et al., "Frequency-stable robust wireless power transfer based on high-order pseudo-Hermitian physics," *Phys. Rev. Lett.*, vol. 130, no. 7, Feb. 2023, Art. no. 077202.

[32] C. Liu, C. Jiang, J. Song, and K. T. Chau, "An effective sandwiched wireless power transfer system for charging implantable cardiac pacemaker," *IEEE Trans. Ind. Electron.*, vol. 66, no. 5, pp. 4108–4117, May 2019.

[33] D. Ahn and S. Hong, "Effect of coupling between multiple transmitters or multiple receivers on wireless power transfer," *IEEE Trans. Ind. Electron.*, vol. 60, no. 7, pp. 2602–2613, Jul. 2013.

Hao Chen was born in Jiangxi, China, in 1999. He received the B.S. degree in electrical engineering from the School of Electrical Engineering and Automation, Nanchang University, Nanchang, China, in 2021. He is currently working toward the M.S. degree in energy dynamics with the School of Electric Power, South China University of Technology, Guangzhou, China.

His current research interests include wireless power transfer applications and power electronics.

Dongyuan Qiu (Senior Member, IEEE) received the B.Sc. and M.Sc. degrees in automation from the South China University of Technology, Guangzhou, China, in 1994 and 1997, respectively, and the Ph.D. degree in electronic engineering from the City University of Hong Kong, Kowloon, Hong Kong, in 2002.

She is currently a Professor with the School of Electric Power, South China University of Technology. She has authored or coauthored four books, more than 100 papers, and holds more than 100 patents. Her main research interests include modeling and control of power electronic converters, wireless power transfer, and fault diagnosis of power electronic systems.

Dr. Qiu is an Associate Editor of the IEEE TRANSACTIONS ON POWER ELECTRONICS.

Chao Rong was born in Shanxi, China, in 1995. He received the B.S. degree in electrical engineering and automation in 2018 from the South China University of Technology, Guangzhou, China, where he is currently working toward the Ph.D. degree in power electronics and power drives.

His current research interests include wireless power transfer technology and fractional-order system.

Bo Zhang (Senior Member, IEEE) was born in Shanghai, China, in 1962. He received the B.S. degree in electrical engineering from Zhejiang University, Hangzhou, China, in 1982, the M.S. degree in power electronics from Southwest Jiaotong University, Chengdu, China, in 1988, and the Ph.D. degree in power electronics from the Nanjing University of Aeronautics and Astronautics, Nanjing, China, in 1994.

He is currently a Professor with the School of Electric Power, South China University of Technology, Guangzhou, China. He has authored or coauthored more than 450 papers and held 102 patents. He has authored eight monographs. His current research interests include nonlinear analysis, modeling and control of power electronic converters, and wireless power transfer applications.